Letter

Quantum transport anomalies in dispersionless quantum states

Alexander Kruchkov
Institute of Physics, Swiss Federal Institute of Technology (EPFL), Lausanne, CH 1015, Switzerland;
Department of Physics, Harvard University, Cambridge, Massachusetts 02138, USA;
and Branco Weiss Society in Science, ETH Zurich, Zurich, CH 8092, Switzerland

(Received 24 March 2023; accepted 4 May 2023; published 12 June 2023)

Dispersionless quantum states ("flat bands") are counterintuitive: with the electron velocity vanishing, our conventional notions of quasiparticle transport are no longer valid. While the standard Drude-Sommerfeld theory predicts vanishing conductivity in trivial dispersionless bands, in the dispersionless topological bands the electronic wave functions entangle leading to unconventional (non-Drude) quantum transport. We here research the quantum transport in topological flat bands, and find that the quantum-geometric (entanglement) contribution gives rise to several quantum transport anomalies. We highlight structurally similar expressions for *strong anomalies* in thermoelectric response and superfluid flow in the flat bands. The thermopower anomaly in topological flat bands is reaching values of the quantum unit of thermopower ($\frac{k_B}{e}\ln 2 \approx 60\ \mu\mathrm{V/k}$)—the behavior commensurate with the thermopower anomalies in twisted bilayer graphene at the magic angle [Nat. Phys. **18**, 290 (2022)].

DOI: 10.1103/PhysRevB.107.L241102

Introduction. The Drude-Sommerfeld model describes the conductivity σ of dispersive electrons in a metal through the notion of effective mass m,

$$\sigma_{xx}^{\text{dispersive}} = \frac{ne^2\tau}{m}, \tag{1}$$

where e is electronic charge, τ is the scattering time, and n is electronic density. The larger is the mass, the lower is the conductivity. More importantly, the Sommerfeld model predicts, correctly, that in most materials at low temperature the thermopower—the material quality responsible for converting heat into electricity—remains very low, namely

$$\Theta^{\text{dispersive}} \ll \frac{k_B}{e}. \tag{2}$$

In this regard, the recent observation of the giant thermopower in twisted bilayer graphene $\Theta \sim \frac{k_B}{e}$ in Ref. [1] presents a conceptual challenge.

The larger is the effective mass, the flatter is the electronic band. Within the band theory, the dispersionless electronic states ("flat bands") are counterintuitive since the effective electronic mass becomes infinite, the quasiparticle velocity vanishes, and the conventional notions of electron transport fail. The perfectly flat electronic bands is a change of paradigm in condensed matter physics. With the discovery of the twisted bilayer graphene [2,3], we know that the dispersionless electronic states are emerging at the magic angle 1.05° [4–7]. It was further understood that the magic-angle flat bands are topological, and host a number of unconventional phases, characterized by strange metallicity [8–10], unconventional superconductivity [3,11], fractional Hall conductance [12], and giant thermopower [1]—untypical for conventional electronic systems.

Together with anomalies in longitudinal and Hall transport, and unconventional superconductivity, the large thermopower in the flat bands of twisted bilayer graphene can be another indicator of unconventional transport mechanism, in particular through quantum geometry. Superconductivity in the topological flat bands is enhanced through the nontriviality of Wannier orbitals [13,14], quantified through the quantum geometric tensor [15,16]

$$\mathfrak{G}_{ij}^{(n)} = \left\langle \partial_{k_i} u_{n\mathbf{k}} \middle| [1 - |u_{n\mathbf{k}}\rangle\langle u_{n\mathbf{k}}|] \middle| \partial_{k_j} u_{n\mathbf{k}} \right\rangle, \tag{3}$$

where $u_{n\mathbf{k}}$ is the associated Bloch state of the nth electronic band, which may or may not be flat. The real part of $\mathcal{G}_{ij} = \mathrm{Re}\mathfrak{G}_{ij}$ is the Fubini-Study metrics describing the geometry of the bands, while the imaginary part $\mathcal{F}_{ij} = -2\mathrm{Im}\mathfrak{G}_{ij}$ is Berry curvature reflecting the topology of the Bloch states. In fact, one encounters quantum geometry in different quantum transport anomalies, ranging from quantum noise, optical conductivity, anomalous Hall effect, unconventional superconductivity, and adjacent topics [14,17–26]. The quantum-geometric superconductivity [14] has a particular important role in twisted bilayer graphene, where it has been shown that the quantum-geometric contribution to the superfluid weight is key at the magic angle [27–30]. There is experimental evidence [31] supporting the theory for quantum-geometric superconductivity in the flat bands; the experiment has been performed on the high-quality sample of twisted bilayer graphene (TBG) with $v_F \approx 10^3$ m/s compared to $v_F \approx 10^6$ m/s of the original monolayer graphene. Yet other anomalies in the topological flat bands,—such as, e.g., giant thermoelectric power at the magic angle [1]—remain to be revisited from the quantum geometric perspective as well.

In this paper we assume the topological bands with perfect flatness (as, e.g., in Ref. [5]), in such case the quantum metrics of dispersionless electronic bands saturates the "trace condition" [32–35]

$$\mathrm{Tr}\,\mathcal{G}_{ij}^{\text{flat}}(\mathbf{k}) = \left|\mathcal{F}_{xy}^{\text{flat}}(\mathbf{k})\right|. \tag{4}$$

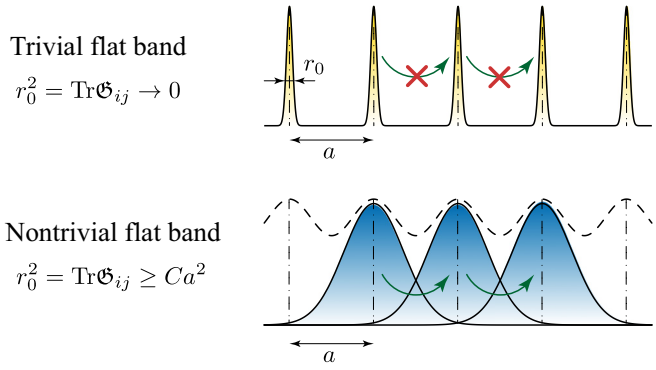

FIG. 1. (Top) In trivial flat bands, electrons are strongly localized (Wannier orbitals sharp) and electronic transport is forbidden; the system is in the insulating phase. (Bottom) In nontrivial flat bands (e.g., Chern bands), the Wannier orbitals cannot be exponentially localized; electrons do not move in the classical sense. Under application of external fields, electrons tunnel between overlapping Wannier orbitals, resulting in unconventional conductivity without electron velocities.

The nontrivial quantum geometry comes at cost such that the electronic Wannier orbitals have a large cross-section [36]. In case of perfectly flat Chern bands (4), the Wannier orbital cross section r_0^2 experiences Lifshitz-Onsager-like quantization [35] with

$$r_0^2 = a^2 \int d\mathbf{k} \mathrm{Tr}\mathcal{G}_{ij}(\mathbf{k}) = a^2 \int d^2\mathbf{k} \mathcal{F}_{xy}(\mathbf{k}) = Ca^2. \quad (5)$$

In other words, the dispersionless electronic states are spread over the atomic lattice, overlapping with C neighboring electronic orbitals, hence allowing quantum tunneling even in the absence of kinetic terms (Fig. 1).

First, we bring to the common denominator different quantum transport anomalies in flat bands before going to the particular discussion on thermopower (since it is calculated through a combination of different quantum transport properties). We show that a generic quantum transport property $\mathfrak{L}_{ij}$ (here $i, j = x, y$) in the flat band material can be expressed through the multiorbital quantum metrics:

$$\mathfrak{L}_{ij}^{\mathrm{flat}} = \sum_{nm,\mathbf{k}} \mathcal{I}_{nm}(\mathbf{k}) \mathrm{Re}\mathfrak{G}_{ij}^{nm}(\mathbf{k}) + \mathcal{J}_{nm}(\mathbf{k}) \mathrm{Im}\mathfrak{G}_{ij}^{nm}(\mathbf{k}),$$

where $\mathfrak{G}_{ij}^{nm}(\mathbf{k}) \equiv \langle \partial_{k_i} u_{n\mathbf{k}} | u_{m\mathbf{k}} \rangle \langle u_{m\mathbf{k}} | \partial_{k_j} u_{n\mathbf{k}} \rangle$ is the generalized quantum-geometric tensor (defined further in text), and $\mathcal{I}_{nm}(\mathbf{k})$ and $\mathcal{J}_{nm}(\mathbf{k})$ are the material structural tensors expressed through quasiparticle propagators further. Note that neither the quasiparticle velocities nor bandwidth enter this expression; this flat-band transport is purely quantum, with its origin in Wannier orbital overlap (Fig. 1). The quantum transport anomalies in $\mathfrak{L}_{ij}^{\mathrm{flat}}$ have no Drude-Sommerfeld counterpart.

Quantum transport formalism for perfectly flat bands. In what follows below we consider a weakly-dispersive Chern band and then set the bandwidth (and hence the Fermi velocity) to *exact zero* [37]. The main result is illustrated for the perfectly flat Chern bands, however, it also applies to all geometrically-nontrivial flat bands (Wannier function are not exponentially localized), thus, including those in twisted bilayer graphene and similar materials.

The derivation of the polarization tensor is rather conventional and can be obtained in several ways. A disciplined way to derive it is through using the current-current correlators in Matsubara framework [38]. The quantum transport properties are computed through imaginary-time Matsubara correlators

$$\mathcal{L}_{ij}^{\alpha\beta}(\tau, \tau') = -\left\langle \mathcal{T}_\tau J_i^\alpha(\tau) Q_j^\beta(\tau') \right\rangle, \quad (6)$$

where Q^α is the generalized "charge" operator (we denote $\alpha = 1$ for electric charge, $\alpha' = 2$ for heat transfer), $i, j = x, y$, and $\mathbf{J}^\alpha$ is the generalized current. For example, for the electric current of charge e, one writes [38]

$$\mathbf{J} = \frac{e}{\hbar} \sum_{\mathbf{k}} c_{\mathbf{k}}^\dagger \frac{\partial \mathcal{H}_{\mathbf{k}}}{\partial \mathbf{k}} c_{\mathbf{k}}. \quad (7)$$

To calculate the response functions $\mathcal{L}_{ij}$, we introduced the auxiliary current-current correlators

$$\Pi_{ij}^{\alpha\beta}(\tau) = -\left\langle \mathcal{T}_\tau J_i^\alpha(\tau) J_j^\beta(0) \right\rangle, \quad (8)$$

so in the frequency representation one has $\mathcal{L}_{ij}(i\omega_n) = \frac{1}{i\omega_n}[\Pi_{ij}(i\omega_n) - \Pi_{ij}(0)]$. To calculate the transport properties (such as conductance $\sigma_{ij} = \mathcal{L}_{ij}^{11}$), we further proceed to analytical continuation of $\Pi_{ij}(i\omega_n)$ and then take the DC limit:

$$\mathcal{L}_{ij}^{\alpha\beta} \equiv \lim_{\omega \to 0} \frac{\Pi_{ij}^{\alpha\beta}(\omega) - \Pi_{ij}^{\alpha\beta}(0)}{i\omega}. \quad (9)$$

The Onsager coefficients $\mathcal{L}_{ij}^{\alpha\beta}$ fully describe the transport properties of an electronic system. Experimentally, the transport measurements across the sample are performed by electric and heat measurements [39,40]. We compute electric conductivity $\sigma_{ij} = \mathcal{L}_{ij}^{11}$, thermal conductivity $\kappa_{ij} = \beta(\mathcal{L}_{ij}^{22} - [L_{ij}^{12}]^2/\mathcal{L}_{ij}^{11})$, and thermoelectric power (Seebeck coefficient) $\Theta = \beta\mathcal{L}_{ii}^{12}/\mathcal{L}_{ii}^{11}$ in the dispersionless electronic bands; here $\beta = 1/T$; e is included in the definition of electric current, Eq. (7). A similar response structure to vector potential $\mathbf{A}$ will imply the finite superfluid weight D_S in the dispersionless bands [41,42].

We start from the electric conductivity, for which we calculate the electric polarization tensor $\Pi_{ij}(\omega)$ (here we drop the superscripts $\alpha\beta$ for brevity); for convenience, below we use $\Pi_{ij}(\omega) = \frac{e^2}{\hbar^2}\tilde{\Pi}_{ij}(\omega)$. Evaluating the current-current correlator (8) with (7) in Matsubara representation gives [43]

$$\tilde{\Pi}_{ij}^{\pm}(i\omega_0) = \frac{1}{2\beta} \sum_{\mathbf{k}} \sum_{i\omega_n'} \mathrm{Tr}\, \mathcal{G}_{\mathbf{k}}(i\omega_n') \frac{\partial \mathcal{H}_{\mathbf{k}}}{\partial k_i} \mathcal{G}_{\mathbf{k}}(i\omega_n' \pm i\omega_0) \frac{\partial \mathcal{H}_{\mathbf{k}}}{\partial k_j},$$

where $\mathcal{G}_{\mathbf{k}}(i\omega')$ is the Matsubara transform of the (renormalized) Green function $\mathcal{G}_{\mathbf{k}}(\tau, \tau') = -\langle \mathcal{T}_\tau c_{\mathbf{k}}^\dagger(\tau) c_{\mathbf{k}}(\tau') \rangle$, where expectation value is taken over the interacting vacuum at temperature T. Here Matsubara frequencies $i\omega_n'$ are fermionic and $i\omega_0$ is bosonic.

The influence of the quantum-geometric tensor can be demonstrated in the following way. The position operator in the Bloch basis is [44]

$$\hat{\mathbf{r}}_{mn} = i\partial_{\mathbf{k}}\delta_{nm} + \langle u_{n\mathbf{k}} | \, i\partial_{\mathbf{k}} \, u_{m\mathbf{k}} \rangle. \quad (10)$$

It follows that the generalized velocity in this basis is given by [18,44]

$$\left[\frac{1}{\hbar}\frac{\partial \mathcal{H}_{\mathbf{k}}}{\partial \mathbf{k}}\right]_{nm} = \mathbf{v}_{n\mathbf{k}}\delta_{nm} + \omega_{nm,\mathbf{k}}\,\langle u_{n\mathbf{k}}|\partial_{\mathbf{k}}u_{m\mathbf{k}}\rangle, \tag{11}$$

where $\mathbf{v}_{n\mathbf{k}} = \frac{\partial \varepsilon_{n\mathbf{k}}}{\partial \hbar \mathbf{k}}$ is the quasiparticle velocity in the band ("Fermi velocity") and $\omega_{nm,\mathbf{k}} = \varepsilon_{n\mathbf{k}} - \varepsilon_{m\mathbf{k}}$ are transition frequencies of the multiorbital system (the second term is called "anomalous velocity" [18]). With the velocity operator (11), the polarization tensor (10) have two terms: the first proportional to the Fermi velocities $\mathcal{O}(\mathbf{v}_{n\mathbf{k}}^2)$, and the second being independent of the band dispersion itself. For illustrative purpose, it is useful to write down the first contribution which has a generic form for the nth band $\sigma^{\text{dispersive}} = \frac{e^2}{\hbar}\sum_n \sum_{\mathbf{k}} \frac{\partial \varepsilon_{n\mathbf{k}}}{\partial k_i}\frac{\partial \varepsilon_{n\mathbf{k}}}{\partial k_i} S_n(\mathbf{k}) = 0$; refer to Eq. (1). The conventional (Drude) conductivity vanishes exactly since the electronic band is perfectly flat, as witnessed in zero Fermi velocity $\partial_{\mathbf{k}}\varepsilon_{n\mathbf{k}} \equiv 0$ in all the Brillouin zone. This is where our conventional intuition comes to an edge.

In contrast, by using Eqs. (9)–(11), we find that there is a quantum-geometric contribution to the DC transport even in the case of perfectly flat bands,

$$\sigma_{ij}^{\text{flat}} = \frac{e^2}{\hbar}\sum_{\mathbf{k}}\sum_{nm} \mathcal{I}_{nm}(\mathbf{k})\,\mathrm{Re}\mathfrak{G}_{ij}^{nm}(\mathbf{k}) + \mathcal{J}_{nm}(\mathbf{k})\,\mathrm{Im}\mathfrak{G}_{ij}^{nm}(\mathbf{k}), \tag{12}$$

where we have introduced the generalized geometric tensor for a multiorbital system [16,45]

$$\mathfrak{G}_{ij}^{nm}(\mathbf{k}) \equiv \langle \partial_{k_i} u_{n\mathbf{k}}|u_{m\mathbf{k}}\rangle\langle u_{m\mathbf{k}}|\partial_{k_j}u_{n\mathbf{k}}\rangle; \tag{13}$$

note that $\sum_{m\neq n}\mathfrak{G}_{ij}^{nm} = \mathfrak{G}_{ij}^{(n)}$, with $\mathfrak{G}_{ij}^{(n)}$, given by formula (3). The structural tensors $\mathcal{I}_{nm}(\mathbf{k})$ and $\mathcal{J}_{nm}(\mathbf{k})$ are fully determined by the quasiparticle propagators; they are defined in the symmetrized form as (see the SM [46])

$$\mathcal{I}_{nm}(\mathbf{k}) = -2\omega_{nm,\mathbf{k}}^2 \int_{-\infty}^{+\infty}\frac{d\omega}{2\pi}\, f'(\omega)\,\mathrm{Im}\mathcal{G}_{n\mathbf{k}}^R(\omega)\mathrm{Im}\mathcal{G}_{m\mathbf{k}}^R(\omega),$$

$$\mathcal{J}_{nm}(\mathbf{k}) = 8\,\omega_{nm,\mathbf{k}}^2 \iint_{-\infty}^{+\infty}\frac{d\omega d\omega'}{(2\pi)^2}\,\frac{f(\omega)\,\mathrm{Im}\mathcal{G}_{n\mathbf{k}}^R(\omega')\mathrm{Im}\mathcal{G}_{m\mathbf{k}}^R(\omega)}{(\omega-\omega')^2},$$

with $\omega_{nm,\mathbf{k}} = \varepsilon_{n\mathbf{k}} - \varepsilon_{m\mathbf{k}}$, and $f(w)$ is the Fermi-Dirac distribution function. Generically, the structural tensors $\mathcal{I}_{nm}$ and $\mathcal{J}_{nm}$ are nonzero and depend on the nature of quasiparticles in the system, described by causal propagators $\mathcal{G}_{m\mathbf{k}}^R(\omega)$. Formula (12) is working for the many-body interacting propagators with *well-defined quasiparticle poles*; the quasiparticle energy bands $\varepsilon_{n\mathbf{k}}$ may or may not have dispersion as such.

Quantum Hall effect. In this key example we focus on the transverse response associated with the perfectly flat Chern bands. The transverse (Hall) conductivity determined through quasiparticle propagators is given by Eq. (12) at $T = 0$ as

$$\sigma_{xy}^{\text{flat}} = \frac{8e^2}{\hbar}\sum_{\mathbf{k}}{\sum_{nm}}' \iint_{-\infty}^{+\infty}\frac{d\omega d\omega'}{(2\pi)^2}\,\frac{\mathrm{Im}\mathcal{G}_{n\mathbf{k}}^R(\omega')\mathrm{Im}\mathcal{G}_{m\mathbf{k}}^R(\omega)}{(\omega-\omega')^2} \times \omega_{nm,\mathbf{k}}^2\,\mathrm{Im}\mathfrak{G}_{xy}^{nm}(\mathbf{k}); \tag{14}$$

the summation index n runs over the occupied bands (below Fermi level ε_F). In the limit when the quasiparticles are well defined, one may use $\mathrm{Im}\mathcal{G}_{n\mathbf{k}}^R(\omega) = \delta_{n\mathbf{k}}/[(\omega-\omega_{n\mathbf{k}}+i\delta_{n\mathbf{k}})(\omega-\omega_{n\mathbf{k}}-i\delta_{n\mathbf{k}})]$; the expression (14) contains integrands with pole singularities and we can resort to residue theorem to evaluate integrals for arbitrary $\delta_{n\mathbf{k}}$, $\delta_{m\mathbf{k}}$ (see the SM [46]). By choosing an appropriate contour, we obtain $\iint_{-\infty}^{+\infty}\frac{\mathrm{Im}\mathcal{G}_{n\mathbf{k}}^R(\omega')\mathrm{Im}\mathcal{G}_{m\mathbf{k}}^R(\omega)}{(\omega-\omega')^2}d\omega d\omega' \simeq \pi^2[\omega_{n\mathbf{k}}-\omega_{m\mathbf{k}}]^{-2}[1+\mathcal{O}(\delta^2)] \approx \pi^2/\omega_{nm,\mathbf{k}}^2$. Using this expression for formula (14), in the limit of well-resolved energy bands ($\delta_{n\mathbf{k}}, \delta_{m\mathbf{k}} \ll \Delta$, where Δ is the band gap), we obtain the established quantum Hall conductance

$$\sigma_{xy}^{\text{flat}} = \frac{e^2}{\hbar}\sum_n{}'\sum_{\mathbf{k}}\mathcal{F}_{xy}^{(n)}(\mathbf{k}) = \frac{e^2}{h}\sum_n{}'C_n, \tag{15}$$

where $\mathcal{F}_{xy}^{(n)}$ is the Berry curvature of the nth band. Thus we obtain the quantum Hall conductance in the form of TKNN invariant [47]. Note that the *quantized nature* of (14) holds in the presence of moderate interactions, provided the renormalized propagators have well-defined quasiparticle poles. Note also, that when the Fermi level is within the flat band, we obtain the (intrinsic) anomalous Hall effect similar to Refs. [18,48]. The influence of quantum geometry on fractional Hall transport in the topological flat bands are detailed in Ref. [34].

Longitudinal conductance. For storytelling, consider the Haldane model [49] on NN and NNN hoppings ($\Lambda = 2$),

$$\mathcal{H}_0 = \sum_i t_0 c_i^\dagger c_i + \sum_{\langle ij\rangle} t_{ij}^{\text{NN}} c_i^\dagger c_j^\dagger + \sum_{\langle\langle ij\rangle\rangle} t_{ij}^{\text{NNN}} c_i^\dagger c_j^\dagger, \tag{16}$$

where we fix t_{ij}^{NN} as real, and $t_{ij}^{\text{NNN}} = t' e^{i\Phi_{ij}}$. Clearly, for $\Phi_{ij} = \pm\pi/2$, the spectrum becomes particlehole symmetric [49]. This yields, upon transformation (1), two perfectly flat bands positioned at $E = \pm E_0$ [35]. The resulting $\mathcal{H}_0^{\text{flat}}$ becomes nonlocal ($\Lambda' = \infty$), though it is possible to truncate it and make the band arbitrarily flat by choosing a corresponding truncation Λ' and minimizing bandwidth (Refs. [17,35]). Hence, by allowing further hopping terms to (16), this model features two dispersionless Chern bands with $C = \pm 1$. By using the flat band Green's function matrix $1/(\omega - \mathcal{H}_0^{\text{flat}})$ and introducing level broadening $i\delta$, we use Eq. (12) to calculate σ_{xx}.

The longitudinal conductance σ_{xx} of the flat bands demonstrates a *weak anomaly* in temperature dependence: We find that quite generically the σ_{xx} conductance has inverse temperature scaling (Fig. 2),

$$\sigma_{xx}^{\text{flat}}(T) \propto \frac{\delta}{T}\sum_{\mathbf{k}}\mathrm{Tr}\,\mathcal{G}_{ij}(\mathbf{k}) \sim \frac{\delta}{T}. \tag{17}$$

This T^{-1} scaling is quite universal, and while the particular numbers depend on the values of δ [Fig. 2(a)], the $\sigma_{xx}^{-1} \sim T$ scaling is seen both for high temperatures ($T \ll \Delta$) and high temperatures ($T \gg \Delta$), [Figs. 3(d) and 3(e)]. Note however, that the overall slope is slightly different for high temperature and low temperature limits. The weak anomaly (17) might or might not be related to observed effects in Refs. [8–10]. However, the anomaly (17) is hidden for dispersive bands, as the Drude terms (1) happen to be stronger ($\sim 1/\delta$). Importantly, in the Quantum Hall systems the residual $\sigma_{xx}^{\text{flat}} \sim \frac{e^2}{\hbar}\mathcal{O}(\delta^1)$ is typically very weak compared to $\sigma_{xy}^{\text{flat}} \sim \frac{e^2}{\hbar}\mathcal{O}(\delta^0)$.

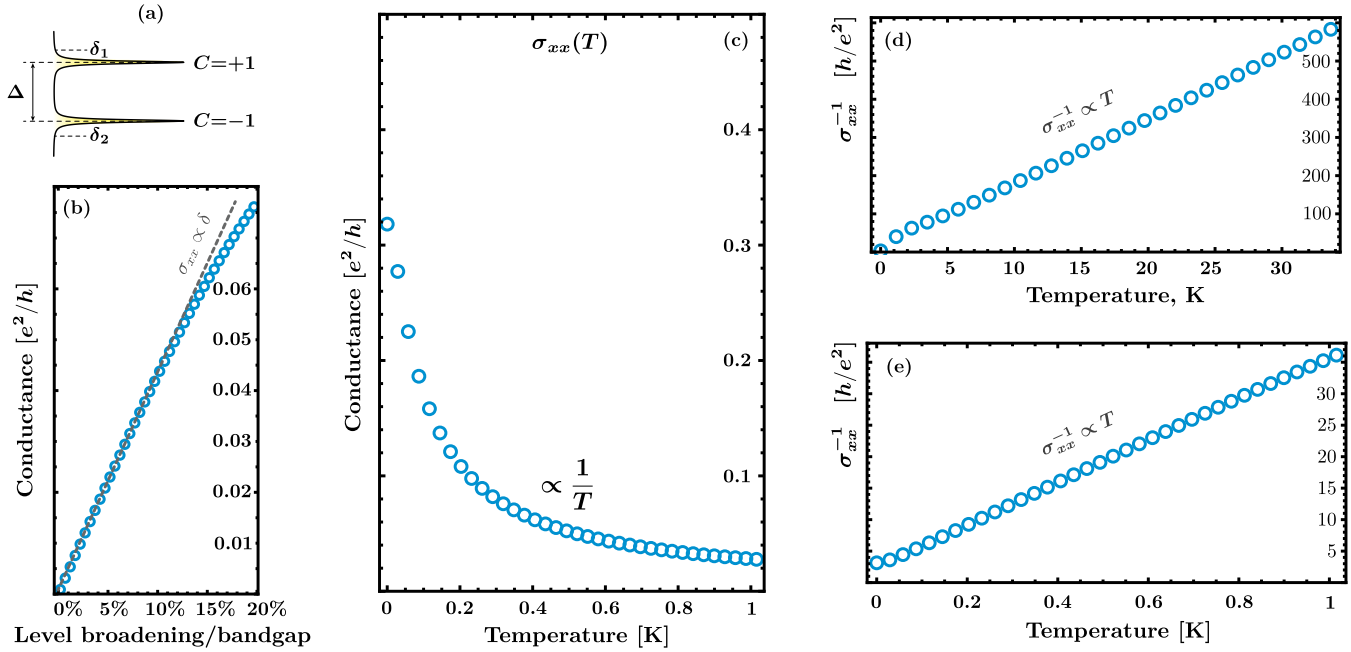

FIG. 2. *Conductivity in topological flat bands.* (a) Schematic of a two-level system with two topological flat bands of $C = \pm 1$. (b) Longitudinal conductance as function of level broadening calculated here for the band gap $\Delta = 0.5$ meV and temperature $T = \Delta$ ($\approx$6 K); here, $\delta_{1,2} \equiv \delta$. (c) Longitudinal conductance as function of temperature, calculated at $\Delta = 0.5$ meV, $\delta_{1,2} = 0.01$ meV. (d), (e) Inverse longitudinal conductance (for the same parameters) shows T-linear scaling both for high temperatures ($T \gg \Delta$) and low temperatures ($T \ll \Delta$); T-slopes in different regimes (d) and (e) are slightly different.

Thermal and thermoelectric response. We further report that the thermoelectric and thermal response have quantum-geometric (entanglement) contributions. In particular, the longitudinal thermal conductance is

$$\kappa_{xx}^{\text{flat}} = \frac{1}{T}\sum_{nm,\mathbf{k}} \mathcal{I}_{nm}^{(2)}(\mathbf{k})\,\text{Re}\mathfrak{G}_{ij}^{nm}(\mathbf{k}) - \frac{1}{T}\frac{\left[\sum_{nm,\mathbf{k}} \mathcal{I}_{nm}^{(1)}(\mathbf{k})\,\text{Re}\mathfrak{G}_{ij}^{nm}(\mathbf{k})\right]^2}{\left[\sum_{nm,\mathbf{k}} \mathcal{I}_{nm}^{(0)}(\mathbf{k})\,\text{Re}\mathfrak{G}_{ij}^{nm}(\mathbf{k})\right]}, \tag{18}$$

and thermoelectric power (Seebeck coefficient) is

$$\Theta_{xx}^{\text{flat}} = \frac{\beta}{e}\frac{\sum_{nm,\mathbf{k}} \mathcal{I}_{nm}^{(1)}(\mathbf{k})\,\text{Re}\mathfrak{G}_{ij}^{nm}(\mathbf{k})}{\sum_{nm,\mathbf{k}} \mathcal{I}_{nm}^{(0)}(\mathbf{k})\,\text{Re}\mathfrak{G}_{ij}^{nm}(\mathbf{k})}, \tag{19}$$

where we have introduced thermoelectric transport tensors

$$\mathcal{I}_{nm}^{(\alpha)}(\mathbf{k}) = -2\omega_{nm,\mathbf{k}}^2 \int \frac{d\omega}{2\pi}\omega^\alpha f'(\omega)\,\text{Im}\mathcal{G}_{n\mathbf{k}}(\omega)\text{Im}\mathcal{G}_{m\mathbf{k}}(\omega).$$

For numerical purposes, we operate with the same flat band model as discussed below Eq. (16), containing two flat Chern bands of band gap Δ and generic level broadening δ_1, δ_2 [Fig. 3(a)]. The thermopower is further calculated via (19) and the dimensional units ($k_B, \hbar$) are restored. We plot the temperature dependence of thermopower for representative parameters parameters $\delta_{1,2} \ll \Delta$ in Fig. 3 (additional plots with different parameters are listed in the SM [46]). The first observation is that the thermopower at the fixed temperature $T \sim \Delta$ is nearly independent of δ [Fig. 2(b)], and thus presents a robust quantum transport observable (in this regard, see also [50] for thermopower in the SYK flat band). This is in contrast to the flat band conductance (Fig. 2), for which we have found $\sigma_{xx} \propto \delta$, and hence being parameter-dependent. The second observation, is that the thermopower is nonmonotonic: it starts nearly linear at low T, but develops a large

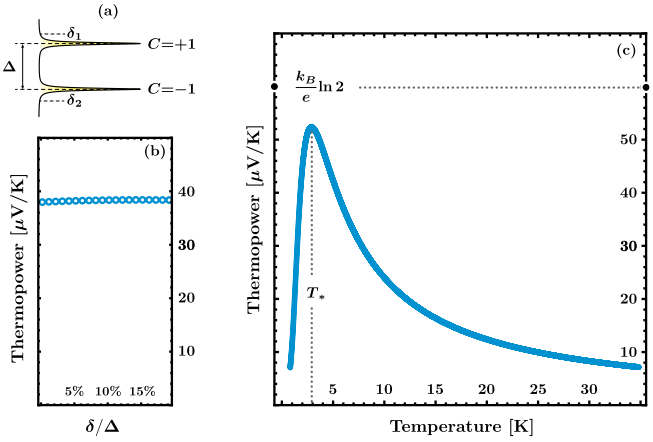

FIG. 3. *Strong thermopower anomaly in topological flat bands.* (a) Schematic of a two-level system with two topological flat bands of $C = \pm 1$. (b) Thermoelectric power Θ as function of level broadening calculated here for the band gap $\Delta = 0.5$ meV and temperature $T = \Delta$ ($\approx$6 K); here, $\delta_{1,2} \equiv \delta$. (c) Thermoelectric power as a function of temperature, plotted here for $\Delta = 0.5$ meV and $\delta_{1,2} = 0.01$. Here thermopower develops a pronounced peak at $T_* \approx \Delta/2$, reaching for some parameters the quantum unit of thermopower $\frac{k_B}{e}\ln 2$. Similar thermopower anomalies had been reported for the magic-angle twisted bilayer graphene [1], where the system features narrow topological bands. Anomaly-free behavior would be described by Eq. (2).

local maximum Θ_*, placed at $T_* \sim \Delta$. The local maximum presents a "giant" thermopower $\sim 50-60\ \mu\mathrm{V/K}$, unexpected for a narrow Bloch band [1]. Above $T_* \sim \Delta$, the thermopower drops to significantly lower values.

In the limit when the level broadening is much smaller than the bandgap, the thermopower associated with dispersionless electronic bands with nontrivial quantum geometry has *strong anomaly* reaching values

$$\Theta_*^{\mathrm{flat}} \simeq \frac{k_B}{e} \ln 2. \tag{20}$$

Compare this thermopower anomaly (20) with the regular dispersive band thermopower (2).

Even a deeper analogy stems here to another case of topological flat bands: in Landau levels [51,52] the value of $\frac{k_B}{e} \ln 2 \approx 60\,\mu\mathrm{V/K}$ sets the quantum unit for thermopower [53]. As thermopower reflects entropy per quasiparticle, the quantum unit $\frac{k_B}{e} \ln 2$ reflects fermionic entropy of $k_B \ln 2$ per electron [54,55], even that there is formally no Planck constant in Eq. (20).

Discussion. In the absence of magnetic fields, thermopower in graphene-based systems remains relatively low ($\ll k_B/e$) unless thermally excited to room temperatures [56,57]. In this regard, observation of thermopower anomaly $\sim k_B/e$ in the flat bands of magic-angle twisted bilayer graphene [1] without magnetic fields was unexpected, not captured by conventional theory, and hence attributed to various interaction effects. However, we remark that two slightly gapped flat bands in TBG at the magic angle can be approximated with Landau level wave functions [5]. Therefore the estimates drawn in this paper for flat band thermopower should qualitatively hold for flat bands in TBG as well. In particular, the observed thermopower anomalies in experiments [1] are consistent with flat band thermopower $\frac{k_B}{e} \ln 2$ (and taking into account the number of flat-band electrons per moiré cell). Moreover, the temperature dependence of thermopower in TBG (Fig. 3(c) in [1]) is consistent with temperature dependence stemming from quantum geometry (Fig. 3).

It is interesting that the superconductivity in perfectly flat Chern bands [13,14] takes origin from the nontrivial quantum metrics as well. In fact, the superfluid weight D_S (defined as a response to external vector potential $\mathbf{A}$) has a similar linear response structure through current-current correlators [20,41], with a difference that $\mathbf{k} \to 0, \omega \to 0$ limits should be taken be with special care [58,59]. In this case, one finds [13]

$$D_S^{\mathrm{flat}} \sim \Delta_S \sum_{\mathbf{k}} \mathrm{Re}\mathfrak{G}_{ii}(\mathbf{k}), \tag{21}$$

where Δ_S is the superfluid gap associated with Bogoliubov-de-Gennes model and its variations [14,20,60]. After a relevant analysis, the result (21) has been applied to twisted bilayer graphene, see Refs. [27–30,61] and Ref.[31], where the quantum geometric contribution to superfluid weight, and hence the $T_{\mathrm{BKT}} \sim \frac{\hbar^2}{e^2} D_S(T=0)$ [62], is argued to be significant. Typically, this mechanism gives $T_{\mathrm{BKT}} \sim 1$ K in TBG.

It would be interesting to build a self-consistent model including both quantum-geometric superconductivity and strange metallicity [63] with both of them stemming from nontrivial $\sum_{\mathbf{k}} \mathrm{Re}\mathfrak{G}_{ij}(\mathbf{k})$.

Acknowledgments. The author thanks Subir Sachdev, Philip Kim, Bertrand Halperin, and Douglas Scalapino for fruitful discussions. This work was financed by the Branco Weiss Society in Science, ETH Zurich through the grant on flat bands, strong interactions, and the SYK physics.

[1] A. K. Paul, A. Ghosh, S. Chakraborty, U. Roy, R. Dutta, K. Watanabe, T. Taniguchi, A. Panda, A. Agarwala, S. Mukerjee *et al.*, Nat. Phys. **18**, 691 (2022).
[2] Y. Cao, V. Fatemi, A. Demir, S. Fang, S. L. Tomarken, J. Y. Luo, J. D. Sanchez-Yamagishi, K. Watanabe, T. Taniguchi, E. Kaxiras *et al.*, Nature (London) **556**, 80 (2018).
[3] Y. Cao, V. Fatemi, S. Fang, K. Watanabe, T. Taniguchi, E. Kaxiras, and P. Jarillo-Herrero, Nature (London) **556**, 43 (2018).
[4] R. Bistritzer and A. H. MacDonald, Proc. Natl. Acad. Sci. USA **108**, 12233 (2011).
[5] G. Tarnopolsky, A. J. Kruchkov, and A. Vishwanath, Phys. Rev. Lett. **122**, 106405 (2019).
[6] S. Lisi, X. Lu, T. Benschop, T. A. de Jong, P. Stepanov, J. R. Duran, F. Margot, I. Cucchi, E. Cappelli, A. Hunter *et al.*, Nat. Phys. **17**, 189 (2021).
[7] The underlying flat bands in TBG can be tuned to perfectly flat [5,64].
[8] H. Polshyn, M. Yankowitz, S. Chen, Y. Zhang, K. Watanabe, T. Taniguchi, C. R. Dean, and A. F. Young, Nat. Phys. **15**, 1011 (2019).
[9] Y. Cao, D. Chowdhury, D. Rodan-Legrain, O. Rubies-Bigorda, K. Watanabe, T. Taniguchi, T. Senthil, and P. Jarillo-Herrero, Phys. Rev. Lett. **124**, 076801 (2020).
[10] A. Jaoui, I. Das, G. Di Battista, J. Díez-Mérida, X. Lu, K. Watanabe, T. Taniguchi, H. Ishizuka, L. Levitov, and D. K. Efetov, Nat. Phys. **18**, 633 (2022).
[11] X. Lu, P. Stepanov, W. Yang, M. Xie, M. A. Aamir, I. Das, C. Urgell, K. Watanabe, T. Taniguchi, G. Zhang *et al.*, Nature (London) **574**, 653 (2019).
[12] Y. Xie, A. T. Pierce, J. M. Park, D. E. Parker, E. Khalaf, P. Ledwith, Y. Cao, S. H. Lee, S. Chen, P. R. Forrester *et al.*, Nature (London) **600**, 439 (2021).
[13] P. Törmä, S. Peotta, and B. A. Bernevig, Nat. Rev. Phys. **4**, 528 (2022).
[14] S. Peotta and P. Törmä, Nat. Commun. **6**, 8944 (2015).
[15] J. Provost and G. Vallee, Commun. Math. Phys. **76**, 289 (1980).
[16] Y.-Q. Ma, S. Chen, H. Fan, W.-M. Liu *et al.*, Phys. Rev. B **81**, 245129 (2010).
[17] T. Neupert, L. Santos, C. Chamon, and C. Mudry, Phys. Rev. Lett. **106**, 236804 (2011).
[18] F. D. M. Haldane, Phys. Rev. Lett. **93**, 206602 (2004).
[19] J.-W. Rhim, K. Kim, and B.-J. Yang, Nature (London) **584**, 59 (2020).
[20] K.-E. Huhtinen, J. Herzog-Arbeitman, A. Chew, B. A. Bernevig, and P. Törmä, Phys. Rev. B **106**, 014518 (2022).
[21] Y. Gao and D. Xiao, Phys. Rev. Lett. **122**, 227402 (2019).

[22] M. F. Lapa and T. L. Hughes, Phys. Rev. B **99**, 121111(R) (2019).
[23] V. Kozii, A. Avdoshkin, S. Zhong, and J. E. Moore, Phys. Rev. Lett. **126**, 156602 (2021).
[24] J. Mitscherling and T. Holder, Phys. Rev. B **105**, 085154 (2022).
[25] J. Ahn, G.-Y. Guo, N. Nagaosa, and A. Vishwanath, Nat. Phys. **18**, 290 (2022).
[26] W. Chen and W. Huang, Phys. Rev. Res. **3**, L042018 (2021).
[27] X. Hu, T. Hyart, D. I. Pikulin, and E. Rossi, Phys. Rev. Lett. **123**, 237002 (2019).
[28] T. Hazra, N. Verma, and M. Randeria, Phys. Rev. X **9**, 031049 (2019).
[29] A. Julku, T. J. Peltonen, L. Liang, T. T. Heikkilä, and P. Törmä, Phys. Rev. B **101**, 060505(R) (2020).
[30] F. Xie, Z. Song, B. Lian, and B. A. Bernevig, Phys. Rev. Lett. **124**, 167002 (2020).
[31] H. Tian, X. Gao, Y. Zhang, S. Che, T. Xu, P. Cheung, K. Watanabe, T. Taniguchi, M. Randeria, F. Zhang *et al.*, Nature (London) **614**, 440 (2023).
[32] S. A. Parameswaran, R. Roy, and S. L. Sondhi, Phys. Rev. B **85**, 241308(R) (2012).
[33] R. Roy, Phys. Rev. B **90**, 165139 (2014).
[34] P. J. Ledwith, G. Tarnopolsky, E. Khalaf, and A. Vishwanath, Phys. Rev. Res. **2**, 023237 (2020).
[35] A. Kruchkov, Phys. Rev. B **105**, L241102 (2022).
[36] N. Marzari and D. Vanderbilt, Phys. Rev. B **56**, 12847 (1997).
[37] If not mentioned otherwise, we work at half-filling.
[38] G. D. Mahan, *Many Particle Physics*, 3rd ed. (Plenum, New York, 2000).
[39] L. Onsager, Phys. Rev. **37**, 405 (1931); **38**, 2265 (1931).
[40] J. Rammer, *Quantum transport theory* (CRC Press, 2018).
[41] E. Rossi, Curr. Opin. Solid State Mater. Sci. **25**, 100952 (2021).
[42] J. Herzog-Arbeitman, A. Chew, K.-E. Huhtinen, P. Törmä, and B. A. Bernevig, arXiv:2209.00007.
[43] We introduce here two quantities $\tilde{\Pi}^{\pm}_{ij}$ in order to evaluate carefully zero-frequency limit in Eq. (9).
[44] E. Blount, in *Solid State Physics* (Elsevier, 1962), Vol. 13 pp. 305–373.
[45] M. Iskin, Phys. Rev. A **105**, 023312 (2022).
[46] See Supplemental Material at http://link.aps.org/supplemental/10.1103/PhysRevB.107.L241102 for quantum transport calculation.
[47] D. J. Thouless, M. Kohmoto, M. P. Nightingale, and M. den Nijs, Phys. Rev. Lett. **49**, 405 (1982).
[48] T. Jungwirth, Q. Niu, and A. H. MacDonald, Phys. Rev. Lett. **88**, 207208 (2002).
[49] F. D. M. Haldane, Phys. Rev. Lett. **61**, 2015 (1988).
[50] A. Kruchkov, A. A. Patel, P. Kim, and S. Sachdev, Phys. Rev. B **101**, 205148 (2020).
[51] S. Girvin and M. Jonson, J. Phys. C **15**, L1147 (1982).
[52] M. Jonson and S. M. Girvin, Phys. Rev. B **29**, 1939 (1984).
[53] We thank Philip Kim for pointing out this observation.
[54] N. Hartman, C. Olsen, S. Lüscher, M. Samani, S. Fallahi, G. C. Gardner, M. Manfra, and J. Folk, Nat. Phys. **14**, 1083 (2018).
[55] K. Yang and B. I. Halperin, Phys. Rev. B **79**, 115317 (2009).
[56] Y. M. Zuev, W. Chang, and P. Kim, Phys. Rev. Lett. **102**, 096807 (2009).
[57] S.-G. Nam, D.-K. Ki, and H.-J. Lee, Phys. Rev. B **82**, 245416 (2010).
[58] D. J. Scalapino, S. R. White, and S. Zhang, Phys. Rev. B **47**, 7995 (1993).
[59] D. J. Scalapino, S. R. White, and S. C. Zhang, Phys. Rev. Lett. **68**, 2830 (1992).
[60] Z. Wang, G. Chaudhary, Q. Chen, and K. Levin, Phys. Rev. B **102**, 184504 (2020).
[61] Y. Guan, O. V. Yazyev, and A. Kruchkov, Phys. Rev. B **106**, L121115 (2022).
[62] D. R. Nelson and J. M. Kosterlitz, Phys. Rev. Lett. **39**, 1201 (1977).
[63] P. W. Phillips, N. E. Hussey, and P. Abbamonte, Science **377**, eabh4273 (2022).
[64] P. San-Jose, J. Gonzalez, and F. Guinea, Phys. Rev. Lett. **108**, 216802 (2012).